Role of the right dorsal anterior insula in the urge to tic in Tourette syndrome

Sule Tinaz, MD, PhD[1], **Patrick Malone, BS**[2], **Mark Hallett, MD**[1], and **Silvina G. Horovitz, PhD**[1]

[1]Human Motor Control Section, National Institute of Neurological Disorders and Stroke, National Institutes of Health, Bethesda, MD, 20892, USA

[2]Office of the Clinical Director, National Institute of Neurological Disorders and Stroke, National Institutes of Health, Bethesda, MD, 20892, USA

Abstract

Background—The mid-posterior part of the insula is involved in processing bodily sensations and urges and is activated during tic generation in Tourette syndrome. The dorsal anterior part of the insula, on the other hand, integrates sensory and emotional information with cognitive valuation, and is implicated in interoception. The right dorsal anterior insula also participates in urge suppression in healthy subjects. The current study examined the role of the right dorsal anterior insula in the urge to tic in Tourette syndrome.

Methods—Resting-state functional magnetic resonance imaging was performed in 13 adult Tourette patients and 13 matched controls. The role of the right dorsal anterior insula within the urge-tic network was investigated using graph theory-based neural network analysis. The functional connectivity of the right dorsal anterior insula was also correlated with urge and tic severity.

Results—Even though the patients did not exhibit any overt tics, the right dorsal anterior insula demonstrated higher connectivity, especially with the frontostriatal nodes of the urge-tic network in patients compared to controls. The functional connectivity between the right dorsal anterior insula and bilateral supplementary motor area also correlated positively with urge severity in patients.

Conclusions—These results suggest that the right dorsal anterior insula is part of the urge-tic network and could influence the urge- and tic-related cortico-striato-thalamic regions even during

rest in Tourette syndrome. It might be responsible for heightened awareness of bodily sensations generating premonitory urges in Tourette syndrome.

Keywords

functional MRI; resting-state; graph theory; network; interoception

Introduction

Tourette syndrome (TS) is a neuropsychiatric disorder characterized by motor and vocal tics and psychiatric comorbidities. Most patients with TS describe unpleasant bodily sensations preceding the tics[1] that are perceived as an urge to act.[2] The pathophysiology of tics in TS is attributed to dysfunction in multiple areas of the cortico-striato-thalamo-cortical (CSTC) circuits.[3] Furthermore, evidence from functional neuroimaging studies suggests a role for the insula in urge,[4] making it an area of interest to understand the urge to tic in TS patients.

Physiological urges have a clear interoceptive source, i.e., the sensory inputs arising within the body especially in the viscera (e.g., urge to urinate, yawn, cough, etc.). We think that tic-related urges are also associated with interoceptive awareness, but the sensory source is unclear. However, urge is separate from the sensation. The sensation that our bladder is full is distinct from the need (urge) to empty it.[5] Therefore, in this study, we focused on the urge to tic regardless of the specific nature of these sensations, and postulated a role for the insula - specifically the dorsal anterior part - in heightened interoceptive awareness leading to the urge to tic.

The insula is involved in processing bodily sensations and interoceptive awareness following a posterior-to-anterior gradient, respectively.[6-9] Neuroimaging studies demonstrated activation of the insula during control or suppression of urges in healthy subjects. A meta-analysis showed activation in the posterior and mid-insula during the urge to urinate, swallow, and yawn.[10] Blink suppression also recruited the posterior and mid-insular cortex,[4,11] as well as the right dorsal anterior insula (dAI).[4]

Insula activity was also observed in studies with TS patients. Overactivation of the posterior and mid-insula together with somatosensory and medial frontal areas was shown consistently throughout tic generation in TS patients.[12,13,14] The primary sensorimotor cortex showed resting-state functional connectivity (FC) with the same insular regions, as well as with the right AI only in TS patients compared to controls.[15] Taken together, these findings suggest a critical role for the posterior and mid-insula in representing premonitory sensations. The AI might be involved in increased awareness of these sensations leading to an urge to tic in TS patients.

We investigated the role of the right dAI in the urge to tic in TS patients. While the ventral AI is involved in affective and emotional processing, the dAI is critical in integrating sensation and emotion with cognitive valuation,[7,16] which would be essential in processing and being aware of the urge. Therefore, we constructed an urge-tic network using the coordinates of brain areas recruited before and at tic onset as nodes.[12] We also added the right dAI that demonstrated robust activity during suppression of urge to blink as a node to

our urge-tic network.[4] We tested this urge-tic network using the resting-state functional magnetic resonance imaging (fMRI) data previously obtained from TS patients and matched controls[15] and examined the behavior of the right dAI within this network using graph theoretical network analysis. We hypothesized that the right dAI would form functional connections with more nodes of the urge-tic network in TS patients compared to controls, and this "aberrant" connectivity would have implications for the urge to tic.

Methods and Materials

Participants

Resting-state fMRI data previously collected from 13 TS patients (age range 18-46 years, 3 females, all right-handed) and 13 matched healthy volunteers (HVs) (age range 22-56 years) were used.[15] The study was approved by the Combined NeuroScience Institutional Review Board of the National Institutes of Health, and all subjects gave informed consent. All subjects had normal neurological examination, normal clinical MRI scans, and no psychiatric conditions (except for tics and comorbid obsessive compulsive disorder and attention deficit hyperactivity disorder in patients). Patients were required to taper and discontinue their psychotropic medications at least two weeks prior to participating in the study. Patients were also assessed using the Yale Global Tic Severity (YGTS) scale[17] and Premonitory Urge for Tics Scale (PUTS).[18]

Imaging data collection

T1-weighted anatomical MRI (MPRAGE, voxel size $1\times1\times1$ mm, repetition time (TR) = 4.964 ms, inversion time (TI) = 725 ms, echo time (TE) = 2 ms, matrix size = 256×256, field of view (FoV) = 240×240 mm) and resting-state fMRI scans for 5 min 10 s with eyes closed (echo planar images (EPI), voxel size: $3.75 \times 3.75 \times 5$ mm, TR=2 s, TE=30 ms, flip angle=70 degrees, matrix=64×64, FoV=240×240 mm) were collected at 3T. A vacuum cushion that molds to the subject's head was used to restrict motion. Subjects were video-monitored for movement throughout scanning using a MRI-compatible electronic view window video system (MRA, Inc.). This system allowed viewing of whole body, neck, and face motion except for eye blinks.

Imaging data analysis

Resting-state fMRI—The resting-state fMRI data were analyzed using the Analysis of Functional Neuroimages (AFNI) software.[19] The afni_proc.py script for preprocessing and @ANATICOR script for artifact detection and removal from resting-state time series were used as previously described.[15,20] We removed the first three EPI volumes and slice time- and motion-corrected the rest of them. Motion limit was 0.4 mm and outlier limit was 0.1 (i.e., 10% of all brain voxels per TR that are above the mean absolute deviation threshold from the polynomial trend). We regressed out the nuisance variables including motion, spikes, and local white matter, normalized the EPI volumes to the MNI_caez_N27 template, and smoothed them with a 6-mm full-width-half-maximum Gaussian kernel. Global signal was not removed. The time series were bandpass-filtered ($0.01 < f < 0.1$ Hz) to capture the resting state fluctuations of the blood oxygenation level-dependent (BOLD) signal.

Mild tics that may have been released during scanning and not detected with video monitoring could be associated with sustained BOLD response in motor regions. To address this potential confound, we computed the mean and standard deviation of the resting state BOLD time courses extracted from the left and right precentral gyrus for each subject and compared the results between the two groups.

Connectivity analysis

Network definitions—In an event-related fMRI study, Bohlhalter et al.[12] reported brain areas that were recruited at tic onset ("tic") and 2 s before tic onset ("urge"). We combined these areas and the right dAI from Berman et al.[4], including it as an urge node, to create a composite urge-tic network and used it in our resting-state dataset. The Talairach coordinates were transformed into the MNI space using the Yale BioImage Suite Package tal2mni tool.[21] We did not include the cerebellar areas because cerebellum was not fully covered within the field of view during EPI acquisition. Bilateral putamen had the same coordinates in both urge and tic conditions and was included only once (Fig. 1A, Table 1, Supplementary Data).

We then extracted the BOLD signal time courses from spheres with a radius of 5 mm centered on each node. A Pearson correlation coefficient was calculated between the BOLD time course of each node and the time course of every other node. The resulting correlation adjacency matrices including all nodes were thresholded at multiple levels of the correlation coefficient "r" ($0.1 \leq r \leq 0.4$ in increments of 0.05) to ensure consistency across multiple thresholds. In this context, these correlation coefficients are called "connections."

Graph Metric Calculation—Graph metrics were calculated using custom MATLAB scripts containing functions from the Brain Connectivity Toolbox.[22] For each node of the urge-tic network, we calculated the degree and node strength as a general measure of connectivity, global efficiency and betweenness centrality as measures of functional integration, and clustering coefficient and local efficiency as measures of functional segregation (Table 2). [22,23]

Between-group differences were assessed using 5000 permutations and a significance level set at $p \leq 0.05$, two-tailed (Mattest function in Bioinformatics toolbox of Matlab 2013a). Thresholds are often arbitrarily determined and networks should ideally be characterized across a broad range of thresholds.[22] For consistency, we considered graph metrics indicating a significant difference ($p \leq 0.05$) between the two groups at a minimum of four out of seven correlation thresholds.

Post-hoc behavioral correlations with network findings—Based on our network findings in dorsomedial frontal nodes and prior reports on the importance of these regions in urge and tic generation,[12,13,29-31] we examined the relationship between behavior and the right dAI – dorsomedial frontal FC.

We extracted the unthresholded and seven thresholded connectivity values between the right dAI and the dorsomedial prefrontal nodes (right SMA1, right SMA2, right SMA3, left SMA1, left SMA2, and left midCG as listed in Table 1) in the TS group. We then correlated

these values with YGTS and PUTS scores using multivariate regression treating connectivity values as dependent variables and behavioral scores as covariates.

Results

Participants

TS patients had a mild-to-moderate tic severity (YGTS objective 21.6 ± 5.4, range 14-32) and a high intensity of premonitory urges (PUTS 30.2 ± 3.7, range 23-36) (Supplementary Data Table 1). Body parts involved in motor tics and number of patients who had these tics were as follows: Eye blinking and other eye movements (N = 8), face (N = 12), head (N = 9), neck and shoulder (N = 6), arm/hand (N = 5), leg/foot/toe (N = 6), abdomen (N = 5). In seven patients, motor tics also had a complex or orchestrated pattern. All patients had simple vocal tics (sounds, noises). Three patients also had complex vocal tics (words, phrases). We did not observe any overt tics during the fMRI scans.

Image preprocessing

The average motion per TR for HVs was 0.10 ± 0.05 mm and for patients 0.06 ± 0.04 mm. The average maximum displacement for HVs was 0.7 ± 0.4 mm and for patients 0.9 ± 0.4 mm. Finally, the average number of censored TRs for HVs was 1.15 ± 2.0 and for patients 3.6 ± 7.1. None of these parameters differed significantly between the groups (two-sample t-tests, respective p values were 0.07, 0.4, and 0.2).

Mean and standard deviation values of the resting state BOLD time courses extracted from the left and right precentral gyrus did not differ significantly between the groups (two-sample t-tests, left precentral gyrus: p for mean and SD = 0.49 and 0.53, respectively; right precentral gyrus: p for mean and SD = 0.86 and 0.99, respectively).

Graph Metrics

All graph metrics were calculated on the final urge-tic network consisting of 35 nodes.

The TS group compared to the HVs showed reduced degree in the left mid-cingulate and right supramarginal gyri; reduced betweenness centrality in the left supplementary motor area (SMA) and right mid-insula; higher degree and node strength in the right thalamus; and higher betweenness centrality in the right dAI (Fig. 1C) and right putamen (Table 3). The global network efficiency was not significantly different between the groups. The differences in clustering and local efficiency did not reach our significance criteria.

Post-hoc behavioral correlations with network findings

We found significant positive correlations between PUTS scores and right dAI – right SMA2 unthresholded connectivity (F = 9.49, t = 3.08, p = 0.012) and between PUTS scores and right dAI – left SMA1 unthresholded connectivity (F = 5.78, t = 2.40, p = 0.037). These correlations also remained significant across all seven connectivity thresholds of these two node pairs. YGTS scores did not correlate significantly with connectivity between any node pair.

Discussion

Our data suggest that even in the absence of overt tics, the urge-tic network exhibits a different FC pattern in TS patients. This pattern seems related to the urge to tic implying that "resting" is a different state for patients compared to HVs.

The significant differences in the degree, node strength, and betweenness centrality metrics between the groups indicate overall decreased connectedness in the dorsomedial frontal nodes and increased connectedness in the striatothalamic and right dAI nodes of the urge-tic network in the TS group.

The role of the right dAI in the urge-tic network

The betweenness centrality was reduced in the right mid-insula and increased in the right dAI in the TS group. Different parts of the insula exhibit distinct anatomical connectivity and functional specialization. The mid-posterior part is involved in somatosensory processing.[26,27] It is also functionally connected to the somatosensory cortex and SMA.[16] The dAI, on the other hand, integrates multimodal sensory, emotional, and cognitive information, and is involved in interoception.[6,7,10,16] Neuroimaging studies of normal bodily urges in healthy subjects and urge/tic in TS patients reported mid-posterior insula activity,[10-13] but not dAI activity. The right dAI activity became manifest only when the hemodynamic response function associated with urge was modeled as a "build-up" prior to action.[4] Our finding of higher betweenness centrality of the right dAI points to a relative anterior shift regarding the bridging role of the insula within the urge-tic network in the TS group. This indicates that the right dAI might be functioning as an abnormal "hub" forming atypical links with additional nodes of the network in the TS group. Based on this, we argue that the perception of bodily sensations and urges associated with tics may be enhanced in TS patients leading to stronger recruitment of the right dAI. The right dAI then relays the increased awareness of bodily sensations and urges to tic to the other nodes of the network via its "aberrant" connections and facilitates tic generation.

In this regard, our frontostriatal findings in the TS group are especially relevant (Fig. 1B) within the framework of the CSTC hypothesis, which has been the prevailing view in TS pathology.[28] Our data are also in line with this view as we discuss next.

Frontal nodes

We found reduced degree in the left mid-cingulate gyrus and reduced betweenness centrality in the left SMA in the TS group. Both of these nodes are involved in tic generation and suppression of tics and voluntary behavior.[12,13,29,30] Activity in the SMA cross-correlated with the primary motor cortex activity before, at, and after tic onset in TS patients.[31] Strong SMA activity during spontaneous tics in TS patients also correlated significantly with tic severity.[32] Resting-state connectivity within SMA also correlated with tic severity.[14] Similarly, the dorsal mid-cingulate cortex has a high probability of anatomical interconnections with premotor and parietal areas overlapping with its role in motor function.[33,34] The anterior and dorsal cingulate regions were recruited during urge and tic suppression in TS patients.[29,30] Here, despite their overall decreased FC, the dorsomedial

frontal nodes demonstrated increased FC with the right dAI in the TS group (Fig 1B) implicating heightened limbic drive on these nodes. Our post-hoc analysis showing positive correlations between the urge severity and right dAI – SMA FC supports this argument. Electrical stimulation of the SMA induces not only movement, but also an urge to move in the absence of overt movement.[35] Insula and SMA also demonstrate robust activation preceding tics [12,14] suggesting a role for these structures and their interaction in premonitory urges.

Striatothalamic nodes

We found increased degree and node strength in the right thalamus and increased betweenness centrality in the right putamen in the TS group.

These findings support evidence for thalamus and basal ganglia pathology in TS. *In vivo* MRI studies demonstrated striatal volume loss in TS [36,37] and post-mortem pathological studies in TS showed neuronal loss in the striatum. Specifically, significant gamma-aminobutyric acid (GABA)-ergic[38,39] and cholinergic neuronal loss in the putamen was demonstrated.[39] In addition, deep brain stimulation of the centromedian-parafascicular complex of the thalamus reduced tics.[40] This complex, as well as the ventral anterior and ventral lateral nuclei, send topographically specific projections to the striatum highlighting the importance of the thalamostriatal system in tic generation.[41]

Neuroimaging studies also provide evidence for thalamus and basal ganglia involvement in tic generation. Putamen and thalamus activity was observed during spontaneous tics.[12,13,14,32] Moreover, tic severity correlated positively with the causal interactions within the CSTC loop consisting of the primary motor cortex, putamen, pallidum and thalamus.[32]

Even though we did not find significant structural volumetric loss in the basal ganglia or the thalamus in the TS group (Supplementary Data Table 2), we cannot rule out specific neuronal loss. For instance, GABAergic neuronal loss in the putamen would result in a decreased inhibitory tone and hypothetically contribute to the aberrant FC of the right putamen, e.g., with the right dAI (Fig 1B), in the TS group.

Taken together, our results are consistent with the CSTC hypothesis demonstrating resting-state changes in the graph metrics of the frontostriatal nodes. Decreased connectedness in the dorsomedial frontal nodes may be related to a baseline deficit in their integration capacity in TS. An intact integration capacity would allow these nodes to monitor and keep the urges and unwanted actions tonically in check. However, a reduced integration capacity would eventually be overwhelmed by the mounting urge and finally allow tic release. Based on our results demonstrating connections between the right dAI and frontostriatal nodes in the TS group, we posit that the right dAI might impose the limbic drive on the dorsomedial frontal nodes by conveying the heightened awareness of bodily sensations to these regions. The highly engaged striatothalamic nodes would then provide the cues facilitating tic release through the "loosened" frontal control gates.

Consistent with its role in awareness, the insula is also part of the mesocorticolimbic reward system and shows drug-cue reactivity in addiction leading to cravings.[42] Indeed, deep

repetitive transcranial magnetic stimulation (rTMS) of the insula combined with exposure to smoking cues was effective in smoking cessation.[43] We think that our findings also have therapeutic implications and propose that stimulating the right dAI, for instance using rTMS, might be a promising treatment strategy to control the urge to tic in TS.

Limitations

We did not include the cerebellum because full cerebellar coverage was not obtained for every subject during scanning. Its role in the urge-tic network should be addressed in future studies.

Though patients were not explicitly told to suppress their tics, every participant was instructed to avoid head motion as much as possible. This standard instruction may have made the patients more self-aware of their urges, and perhaps even suppress their tics, which raises the question whether there is a true resting-state in TS. Nevertheless, the intensity of premonitory urges at rest and the capacity to inhibit the tics do not correlate and seem to have different neural mechanisms.[44-46]

Our network approach should be applied to actual tic-related brain activity to delineate the role of different nodes in the network and shed more light on the pathophysiology of tics.

Supplementary Material

Refer to Web version on PubMed Central for supplementary material.

Acknowledgments

References

1. Leckman JF, Walker DE, Cohen DJ. Premonitory urges in Tourette's syndrome. Am J Psychiatry. 1993; 150:98–102. [PubMed: 8417589]

2. Kwak C, Dat Vuong K, Jankovic J. Premonitory sensory phenomenon in Tourette's syndrome. Mov Disord. 2003; 18:1530–1533. [PubMed: 14673893]

3. Leckman JF, Riddle MA. Tourette's syndrome: when habit-forming systems form habits of their own? Neuron. 2000; 28:349–354. [PubMed: 11144345]

4. Berman BD, Horovitz SG, Morel B, Hallett M. Neural correlates of blink suppression and the buildup of a natural bodily urge. Neuroimage. 2012; 59:1441–1150. [PubMed: 21906689]

5. Belluscio BA, Tinaz S, Hallett M. Similarities and differences between normal urges and the urge to tic. Cogn Neurosci. 2011; 2(3-4):245–246. [PubMed: 24168545]

6. Craig AD. How do you feel--now? The anterior insula and human awareness. Nat Rev Neurosci. 2009; 10:59–70. [PubMed: 19096369]

7. Kurth F, Zilles K, Fox PT, Laird AR, Eickhoff SB. A link between the systems: functional differentiation and integration within the human insula revealed by meta-analysis. Brain Struct Funct. 2010; 214:519–534. [PubMed: 20512376]

8. Simmons WK, Avery JA, Barcalow JC, Bodurka J, Drevets WC, Bellgowan P. Keeping the body in mind: insula functional organization and functional connectivity integrate interoceptive, exteroceptive, and emotional awareness. Hum Brain Mapp. 2013; 34:2944–2958. [PubMed: 22696421]

9. Wiebking C, Duncan NW, Tiret B, et al. GABA in the insula - a predictor of the neural response to interoceptive awareness. Neuroimage. 2014; 86:10–18. [PubMed: 23618604]

10. Jackson SR, Parkinson A, Kim SY, Schüermann M, Eickhoff SB. On the functional anatomy of the urge-for-action. Cogn Neurosci. 2011; 2:227–243. [PubMed: 22299020]

11. Lerner A, Bagic A, Hanakawa T, et al. Involvement of insula and cingulate cortices in control and suppression of natural urges. Cereb Cortex. 2009; 19:218–223. [PubMed: 18469316]

12. Bohlhalter S, Goldfine A, Matteson S, et al. Neural correlates of tic generation in Tourette syndrome: an event-related functional MRI study. Brain. 2006; 129:2029–2037. [PubMed: 16520330]

13. Lerner A, Bagic A, Boudreau EA, et al. Neuroimaging of neuronal circuits involved in tic generation in patients with Tourette syndrome. Neurology. 2007; 68:1979–1987. [PubMed: 17548547]

14. Neuner I, Werner CJ, Arrubla J, et al. Imaging the where and when of tic generation and resting state networks in adult Tourette patients. Front Hum Neurosci. 2014; 8:362. [PubMed: 24904391]

15. Tinaz S, Belluscio BA, Malone P, van der Veen JW, Hallett M, Horovitz SG. Role of the sensorimotor cortex in tourette syndrome using multimodal imaging. Hum Brain Mapp. 2014; 35(12):5834–5846. [PubMed: 25044024]

16. Chang LJ, Yarkoni T, Khaw MW, Sanfey AG. Decoding the role of the insula in human cognition: functional parcellation and large-scale reverse inference. Cereb Cortex. 2013; 23:739–749. [PubMed: 22437053]

17. Leckman JF, Riddle MA, Hardin MT, et al. The Yale Global Tic Severity Scale: initial testing of a clinician-rated scale of tic severity. J Am Acad Child Adolesc Psychiatry. 1989; 28:566–573. [PubMed: 2768151]

18. Woods DW, Piacentini J, Himle MB, Chang S. Premonitory Urge for Tics Scale (PUTS): initial psychometric results and examination of the premonitory urge phenomenon in youths with Tic disorders. J Dev Behav Pediatr. 2005; 26:397–403. [PubMed: 16344654]

19. Cox RW. AFNI: software for analysis and visualization of functional magnetic resonance neuroimages. Comput Biomed Res. 1996; 29:162–173. [PubMed: 8812068]

20. Jo HJ, Gotts SJ, Reynolds RC, et al. Effective Preprocessing Procedures Virtually Eliminate Distance-Dependent Motion Artifacts in Resting State FMRI. J Appl Math. 2013; doi: 10.1155/2013/935154

21. Lacadie CM, Fulbright RK, Rajeevan N, Constable RT, Papademetris X. More accurate Talairach coordinates for neuroimaging using non-linear registration. Neuroimage. 2008; 42:717–725. [PubMed: 18572418]

22. Rubinov M, Sporns O. Complex network measures of brain connectivity: uses and interpretations. Neuroimage. 2010; 52:1059–1069. [PubMed: 19819337]

23. Bullmore E, Sporns O. Complex brain networks: graph theoretical analysis of structural and functional systems. Nat Rev Neurosci. 2009; 10:186–198. [PubMed: 19190637]

24. Jacomy M, Venturini T, Heymann S, Bastian M. ForceAtlas2, a continuous graph layout algorithm for handy network visualization designed for the Gephi software. PLoS One. 2014; 9:e98679. [PubMed: 24914678]

25. Xia M, Wang J, He Y. BrainNet Viewer: a network visualization tool for human brain connectomics. PLoS One. 2013; 8:e68910. [PubMed: 23861951]

26. Craig AD. Interoception: the sense of the physiological condition of the body. Curr Opin Neurobiol. 2003; 13:500–505. [PubMed: 12965300]

27. Ostrowsky K, Magnin M, Ryvlin P, Isnard J, Guenot M, Mauguière F. Representation of pain and somatic sensation in the human insula: a study of responses to direct electrical cortical stimulation. Cereb Cortex. 2002; 12:376–385. [PubMed: 11884353]

28. Leckman JF, Bloch MH, Smith ME, Larabi D, Hampson M. Neurobiological substrates of Tourette's disorder. J Child Adolesc Psychopharmacol. 2010; 20:237–247. [PubMed: 20807062]

29. Peterson BS, Skudlarski P, Anderson AW, et al. A functional magnetic resonance imaging study of tic suppression in Tourette syndrome. Arch Gen Psychiatry. 1998; 55:326–333. [PubMed: 9554428]

30. Mazzone L, Yu S, Blair C, et al. An FMRI study of frontostriatal circuits during the inhibition of eye blinking in persons with Tourette syndrome. Am J Psychiatry. 2010; 167:341–349. [PubMed: 20080981]

31. Hampson M, Tokoglu F, King RA, Constable RT, Leckman JF. Brain areas coactivating with motor cortex during chronic motor tics and intentional movements. Biol Psychiatry. 2009; 65:594–599. [PubMed: 19111281]

32. Wang Z, Maia TV, Marsh R, Colibazzi T, Gerber A, Peterson BS. The neural circuits that generate tics in Tourette's syndrome. Am J Psychiatry. 2011; 168:1326–1337. [PubMed: 21955933]

33. Beckmann M, Johansen-Berg H, Rushworth MF. Connectivity-based parcellation of human cingulate cortex and its relation to functional specialization. J Neurosci. 2009; 29:1175–1190. [PubMed: 19176826]

34. Torta DM, Cauda F. Different functions in the cingulate cortex, a meta-analytic connectivity modeling study. Neuroimage. 2011; 56:2157–2172. [PubMed: 21459151]

35. Fried I, Katz A, McCarthy G, et al. Functional organization of human supplementary motor cortex studied by electrical stimulation. J Neurosci. 1991; 11(11):3656–3666. [PubMed: 1941101]

36. Peterson BS, Thomas P, Kane MJ, et al. Basal Ganglia volumes in patients with Gilles de la Tourette syndrome. Arch Gen Psychiatry. 2003; 60:415–424. [PubMed: 12695320]

37. Bloch MH, Leckman JF, Zhu H, Peterson BS. Caudate volumes in childhood predict symptom severity in adults with Tourette syndrome. Neurology. 2005; 65:1253–1258. [PubMed: 16247053]

38. Kalanithi PS, Zheng W, Kataoka Y, et al. Altered parvalbumin-positive neuron distribution in basal ganglia of individuals with Tourette syndrome. Proc Natl Acad Sci U S A. 2005; 102:13307–13312. [PubMed: 16131542]

39. Kataoka Y, Kalanithi PS, Grantz H, et al. Decreased number of parvalbumin and cholinergic interneurons in the striatum of individuals with Tourette syndrome. J Comp Neurol. 2010; 518:277–291. [PubMed: 19941350]

40. Ackermans L, Neuner I, Temel Y, Duits A, Kuhn J, Visser-Vandewalle V. Thalamic deep brain stimulation for Tourette syndrome. Behav Neurol. 2013; 27:133–138. [PubMed: 23242353]

41. Harris K, Singer HS. Tic disorders: neural circuits, neurochemistry, and neuroimmunology. J Child Neurol. 2006; 21:678–689. [PubMed: 16970869]

42. Jasinska AJ, Stein EA, Kaiser J, Naumer MJ, Yalachkov Y. Factors modulating neural reactivity to drug cues in addiction: a survey of human neuroimaging studies. Neurosci Biobehav Rev. 2014; 38:1–16. [PubMed: 24211373]

43. Dinur-Klein L, Dannon P, Hadar A, et al. Smoking cessation induced by deep repetitive transcranial magnetic stimulation of the prefrontal and insular cortices: a prospective, randomized controlled trial. Biol Psychiatry. 2014; 76:742–749. [PubMed: 25038985]

44. Ganos C, Kahl U, Schunke O, et al. Are premonitory urges a prerequisite of tic inhibition in Gilles de la Tourette syndrome? J Neurol Neurosurg Psychiatry. 2012; 83:975–978. [PubMed: 22842713]

45. Ganos C, Kahl U, Brandt V, et al. The neural correlates of tic inhibition in Gilles de la Tourette syndrome. Neuropsychologia. 2014; 65:297–301. [PubMed: 25128587]

46. Müller-Vahl KR, Riemann L, Bokemeyer S. Tourette patients' misbelief of a tic rebound is due to overall difficulties in reliable tic rating. J Psychosom Res. 2014; 76:472–476. [PubMed: 24840142]

Fig. 1.

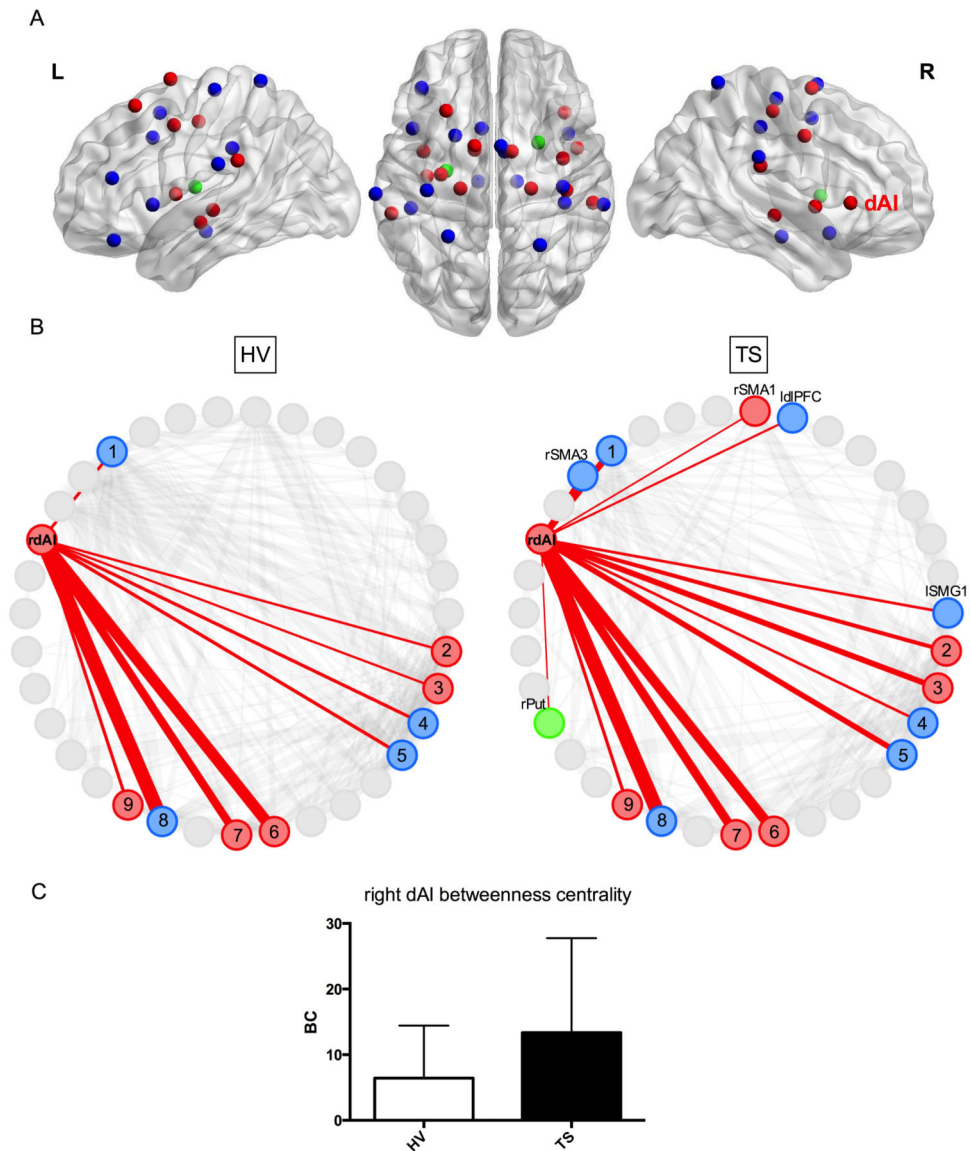**A**. Locations of the urge-tic network nodes are displayed on left (L) and right (R) hemisphere sagittal images and an axial image (middle) based on the MNI template (Gephi[24]). See Table 1 for MNI coordinates. dAI: Dorsal anterior insula. Blue: Tic nodes, red: Urge nodes, green: Urge and tic nodes.

1B. Connectivity pattern of the right dAI (rdAI) is shown at a correlation threshold of r = 0.25 for both groups. This threshold was chosen arbitrarily for display purposes. The thickness of the red lines represents the correlation strengths between the nodes (BrainNet Viewer[25]).

HV: The rdAI showed connections with 1: Left mid-cingulate gyrus, 2, 5: Right supramarginal gyrus (SMG), 3: Left SMG, 4: Right supplementary motor area (SMA), 6: Right mid-insula (MI), 7: Left MI, 8: Left frontal operculum, and 9: Left posterior insula.

TS: The rdAI showed connections with the same nodes as in the HV group, as well as with additional right SMA and left SMG nodes, and unique connections with the left dorsolateral prefontal cortex (ldlPFC) and right putamen (rPut).

1C. The bar graphs demonstrate the betweenness centrality measures of the rdAI at r = 0.25 for each group (HV: White, TS: Black, error bars: Standard deviation, BC: Betweenness centrality). TS group showed significantly higher betweenness centrality in the rdAI compared to the HV group (p = 0.05). This difference was significant across four correlation thresholds (r = 0.1, 0.25, 0.3, and 0.35).

Table 1

MNI coordinates and Brodmann area (BA) labels of nodes

	BA	x	y	z
Urge				
R SMA1	6	10	0	67
L SMA1	6	-11	3	72
L SMA2	6	-11	1	46
L preCG1	6	-30	-13	48
L MFG1	8	-27	23	57
R preCG1	6	39	-4	40
R preCG2	4	41	-22	54
R SMG1	40	56	-29	23
L SMG2	40	-58	-35	26
R Mid-insula 1	13	47	2	0
L Mid-insula	13	-40	0	7
L Posterior insula	13	-38	-14	-9
R dAI	13	40	22	2
R Thalamus (VPL)		21	-21	-5
L Thalamus (VPL)		-19	-21	-2
Tic				
R SMA2	6	4	3	69
R SMA3	6	6	0	50
L midCg	32	-7	13	39
L IFG (p. Orb)	47	-41	35	-19
L dlPFC	46	-41	36	16
L MFG2	6	-22	9	53
L preCG2	6	-38	-22	66
R preCG3	6	39	-20	61
RpostCG	1	40	-29	45
L SMG1	40	-67	-24	24
R SMG2	40	62	-30	28
L SMG3	40	-47	-32	33
R SPL	7	26	-53	70
L SPL	7	-26	-48	71
R Mid-insula 2	13	42	10	-15
L Frontal operculum	44	-46	13	1
R Substantia nigra		13	-17	-17
L Substantia nigra		-9	-17	-14
Urge and Tic				
L Putamen		-27	-11	11
R Putamen		25	5	6

The right dAI node was derived from Berman et al.[4] All other nodes were extracted from Bohlhalter et al.[12] MNI: Montreal Neurological Institute, L: Left, R: Right, dl: Dorsolateral, SMA: Supplementary motor area, midCg: Mid-cingulate gyrus, preCG: Precentral gyrus, postCG: Postcentral

gyrus, PFC: Prefrontal cortex, MFG: Middle frontal gyrus, IFG: Inferior frontal gyrus, p. Orb: Pars orbitalis, SMG: Supramarginal gyrus, SPL: Superior parietal lobule, dAI: Dorsal anterior insula, VPL: Ventral posterolateral nucleus.

Table 2

Graph metric definitions

Functional segregation of a neural network refers to its ability for specialized processing within clusters of nodes.

Functional integration is related to a neural network's ability to bind information efficiently from distributed regions.

Degree is the number of connections that link a node to the rest of the nodes in the network.

Node strength is computed as the sum of weights of the connections that link a node to the rest of the nodes. It indicate show strongly one node is connected to the rest of the nodes in the network.

Path is the shortest distance (i.e., minimum number of connections) between a node and every other node in the network. Efficiency is inversely related to path length.

Global efficiency is calculated as the inverse of the average shortest path length between all pairs of nodes in the network. It is a measure of functional integration.

Node Betweenness Centrality indicates how central a node is to the communication among other nodes in the network. It is computed as the fraction of all shortest paths in the network that contain a given node. Nodes with high values of betweenness centrality participate in a large number of shortest paths and potentially function as hubs.

Clustering coefficient is computed as the number of connections that exist between the nearest neighbors of a node as a proportion of the maximum number of possible connections. It measures the density of connections between neighboring nodes. High clustering is associated with high local efficiency of information transfer.

Local efficiency is computed as the inverse of the average shortest path connecting all neighbors of a node. It reflects how relevant a node is for the communication among other nodes within a local neighborhood, and is related to the clustering coefficient.

Table 3

Changes in graph metrics in TS compared with HV

	Degree	Node Strength	Betweenness
Urge	R Thalamus↑ *	R Thalamus↑ *	RdAI↑
			R Mid-insula 1↓
			L SMA2↓ *
Tic	L midCg↓	-	
	R SMG2↓		
Urge and Tic			R Putamen↑ *

The arrows display the significant changes in graph metrics in TS relative to the HV group. The node labels were determined based on the MNI probabilistic maps in AFNI. L: Left, R: Right, dAI: Dorsal anterior insula, SMA: Supplementary motor area, midCg: Mid-cingulate gyrus, SMG: Supramarginal gyrus.

*
: p   0.05 at five out of seven correlation thresholds. For all other nodes, p   0.05 across four correlation thresholds.